

Charge and spin response functions on a quantum computer: applications to molecules

Taichi Kosugi and Yu-ichiro Matsushita

*Laboratory for Materials and Structures, Institute of Innovative Research,
Tokyo Institute of Technology, Yokohama 226-8503, Japan*

(Dated: November 4, 2019)

We propose a scheme for the construction of charge and spin linear-response functions of an interacting electronic system via quantum phase estimation and statistical sampling on a quantum computer. By using the unitary decomposition of electronic operators for avoiding the difficulty due to their non-unitarity, we provide the circuits equipped with ancillae for probabilistic preparation of qubit states on which the necessary non-unitary operators have acted. We perform simulations of such construction of the response functions for C_2 and N_2 molecules by comparing with the accurate ones based on the full configuration interaction calculations. It is found that the accurate detection of subtle structures coming from the weak poles in the response functions requires a large number of measurements.

I. INTRODUCTION

Since the information carrier of a programmable quantum computer is a set of qubits that exploits the principle of superposition, essentially parallel algorithms can exist and perform computation for classically formidable problems.[1, 2] Quantum chemistry[3] is believed to be one of the most suitable research fields for quantum computation since its problem setting is quantum mechanical by definition. Indeed, a quantum computer can treat a many-electron state composed of lots of Slater determinants as it is in a sense that the electronic state is encoded as a superposition of qubit states via an appropriately chosen map such as the Jordan–Wigner (JW)[4] and Bravyi–Kitaev (BK)[5] transformations.

The quantity which a quantum chemistry calculation is asked to first provide is the total energy of a target system.[6] One of the most widespread methods for obtaining the total energy is the variational quantum eigensolver (VQE), in which a trial many-electron state is prepared via a parametrized quantum circuit. The parameters are optimized iteratively with the aid of a classical computer aiming at the ground state. This approach was first realized[7] by using a quantum photonic device, after which the realizations by superconducting[8, 9] and ion trap[10] quantum computers have been reported. There exist algorithms for obtaining the energy spectra of excited states.[11–16]

Not only academic interest but also industrial demands for accurate explanations and predictions of material properties make it an urgent task to develop methodologies on quantum computers for various electronic properties other than energy levels. The one-particle Green’s functions (GFs) are important in correlated electronic systems[17, 18] since they are often used in explanation of spectra measured in photoemission and its inverse experiments. Recently we proposed a method for the GFs via statistical sampling[19] by employing quantum phase estimation (QPE).[1] Endo et al.,[20] on the other hand, proposed a method for the GFs by focusing on noisy intermediate-scale quantum (NISQ) devices.

The charge and spin response functions χ , formulated in the linear-response theory,[21, 22] describe the leading contributions to the electric and magnetic excitations when perturbation fields are applied to a target system. Since the response functions are the fundamental building blocks in constructing the elaborated methods for correlated electrons such as *GW* theory,[21, 23] the accurate calculation of them is needed.

Given the recent rapid development of fabrication techniques for quantum hardware and the growing demands for quantum computation in material science, it is worth making tools for analyses on correlation effects. In this study, we propose a scheme for the construction of the response functions of an interacting electronic system via statistical sampling on a quantum computer. For examining the validity of our scheme, we perform simulations of such construction of the response functions of diatomic molecules by referring to the full configuration interaction (FCI) results.

This paper is organized as follows. In Section II, we explain the basic ideas and our scheme in detail by providing the quantum circuits for obtaining the response functions via statistical sampling. In Section III, we describe the computational details for our simulations on a classical computer. In Section IV, we show the simulation results for C_2 and N_2 molecules. In Section V, we provide the conclusions.

II. METHODS

A. Definitions

1. Charge and spin response functions

We work with the n_{orbs} orthonormalized spatial orbitals for each spin direction in a target N -electron system, which we assume is in the ground state $|\Psi_{\text{gs}}\rangle$ at zero temperature. The formalism described below can be easily extended to a system with multiple ground states

and/or a nonzero temperature.

By using the creation $a_{p\sigma}^\dagger$ and annihilation $a_{p\sigma}$ operators for the p th spatial orbital of σ spin ($\sigma = \alpha, \beta$), the electron number operator is given by $n_{p\sigma} = a_{p\sigma}^\dagger a_{p\sigma}$. The spin operator is given by $\mathbf{s}_p = \sum_{\sigma, \sigma'} a_{p\sigma}^\dagger (\boldsymbol{\sigma}_{\sigma\sigma'}^{\text{el}}/2) a_{p\sigma'}$, where $\boldsymbol{\sigma}^{\text{el}}$ is the Pauli matrix for the electronic state.

The response functions in terms of charge and spin in time domain for $\mu, \mu' = n, x, y, z$ are defined as^[21]

$$\chi_{p\mu, p'\mu'}(t, t') \equiv -i\theta(t - t') \langle [\mathcal{O}_{p\mu}(t), \mathcal{O}_{p'\mu'}(t')] \rangle. \quad (1)$$

$\mathcal{O}_{p\mu}(t)$ is the operator in the Heisenberg picture for $\mathcal{O}_{pn} \equiv \sum_{\sigma} n_{p\sigma}$ and $\mathcal{O}_{pj} \equiv s_{pj}$ ($j = x, y, z$). To rewrite the expression for the response functions into a more tractable form, we define the charge-charge transition matrix element

$$N_{\lambda p\sigma, p'\sigma'} \equiv \langle \Psi_{\text{gs}} | n_{p\sigma} | \Psi_{\lambda} \rangle \langle \Psi_{\lambda} | n_{p'\sigma'} | \Psi_{\text{gs}} \rangle \quad (2)$$

for the λ th energy eigenstate $|\Psi_{\lambda}\rangle$ of the N -electron states. We define similarly the spin-spin one

$$S_{\lambda pj, p'j'} \equiv \langle \Psi_{\text{gs}} | s_{pj} | \Psi_{\lambda} \rangle \langle \Psi_{\lambda} | s_{p'j'} | \Psi_{\text{gs}} \rangle \quad (3)$$

for $j, j' = x, y, z$ and the spin-charge one

$$M_{\lambda pj, p'\sigma'} \equiv \langle \Psi_{\text{gs}} | s_{pj} | \Psi_{\lambda} \rangle \langle \Psi_{\lambda} | n_{p'\sigma'} | \Psi_{\text{gs}} \rangle \equiv M_{\lambda p'\sigma', pj}^* \quad (4)$$

From these matrix elements, we define the following Hermitian matrices L_{λ} :

$$L_{\lambda pn, p'n} \equiv \sum_{\sigma, \sigma'} N_{\lambda p\sigma, p'\sigma'} \quad (5)$$

$$L_{\lambda pj, p'j'} \equiv S_{\lambda pj, p'j'} \quad (6)$$

$$L_{\lambda pj, p'n} \equiv \sum_{\sigma} M_{\lambda pj, p'\sigma} \quad (7)$$

which are involved in the Lehmann summation over the N -electron energy eigenstates

$$R_{p\mu, p'\mu'}(z) \equiv \sum_{\lambda} \frac{L_{\lambda p\mu, p'\mu'}}{z - (E_{\lambda}^N - E_{\text{gs}}^N)} \quad (8)$$

for a complex frequency z . E_{gs}^N is the ground-state energy and E_{λ}^N is the energy eigenvalue of $|\Psi_{\lambda}\rangle$. Since the response functions defined in eq. (1) depend on time only via $t - t'$ in this case, their expressions in frequency domain are written as

$$\chi_{p\mu, p'\mu'}(\omega) = R_{p\mu, p'\mu'}(\omega + i\delta) + R_{p'\mu', p\mu}(-\omega - i\delta) \quad (9)$$

for a real frequency ω . The positive infinitesimal constant δ appears due to the retarded nature of the response functions, rendering all the poles immediately below the real axis. It is clear that the real part of $\chi_{p\mu, p'\mu'}(\omega)$ is even with respect to ω , while the imaginary part is odd.

2. Unitary decomposition of electronic operators

Although there are alternatives for mapping the electronic operators of a target system to the qubit ones such as JW^[4] and BK^[5] transformations, we do not distinguish between an electronic operator and its corresponding qubit representation in what follows since no confusion will occur for the readers.

For each combination of a spatial orbital p and a spin σ , we can define the following operators for the qubits:^[19]

$$U_{0p\sigma} = a_{p\sigma} + a_{p\sigma}^\dagger \quad (10)$$

and

$$U_{1p\sigma} = a_{p\sigma} - a_{p\sigma}^\dagger, \quad (11)$$

which are unitary regardless of the adopted qubit representation thanks to the anti-commutation relation between the electronic operators and can thus be implemented as logic gates in the quantum computer. This means that we can prepare at least probabilistically an electronic state on which an arbitrary product of the creation and annihilation operators has acted, similarly to the case for GFs.^[19]

In what follows, we assume that the many-electron ground state $|\Psi_{\text{gs}}\rangle$ is already known and can be prepared on a quantum computer.

B. Charge-charge contributions

Let us first consider the determination of the charge-charge transition matrices N_{λ} .

1. Circuits for diagonal components

From the unitary operators in eqs. (10) and (11) for a combination of a spatial orbital p and a spin σ , we define

$$U_{\kappa\kappa'\sigma}^{(p)} \equiv U_{\kappa p\sigma} U_{\kappa' p\sigma} \quad (12)$$

for $\kappa, \kappa' = 0, 1$, which are also unitary. With them, the electron number operator is written as

$$n_{p\sigma} = \frac{U_{00\sigma}^{(p)} + U_{01\sigma}^{(p)} - U_{10\sigma}^{(p)} - U_{11\sigma}^{(p)}}{4}, \quad (13)$$

while the hole number operator is written as

$$\tilde{n}_{p\sigma} \equiv 1 - n_{p\sigma} = \frac{U_{00\sigma}^{(p)} - U_{01\sigma}^{(p)} + U_{10\sigma}^{(p)} - U_{11\sigma}^{(p)}}{4}. \quad (14)$$

We construct a circuit $\mathcal{C}_{p\sigma}$ equipped with two ancillary qubits $|q_0^A\rangle$ and $|q_1^A\rangle$ by implementing the controlled operations of $U_{\kappa\kappa'\sigma}^{(p)}$, as depicted in Fig. 1. The whole system consists of the ancillae and an arbitrary input

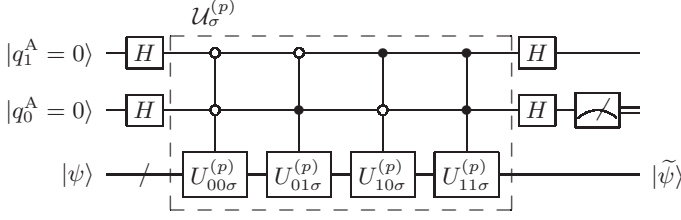


FIG. 1. Charge-charge diagonal circuit $\mathcal{C}_{p\sigma}$ ($\sigma = \alpha, \beta$) for probabilistic preparation of $n_{p\sigma}|\psi\rangle$ and $\tilde{n}_{p\sigma}|\psi\rangle$ from an arbitrary input state $|\psi\rangle$ and two ancillary qubits. H in the circuit represents the Hadamard gate. We define the partial circuit $\mathcal{U}_\sigma^{(p)}$ by enclosing it with dashed lines.

register $|\psi\rangle$. Its state changes by undergoing the circuit as

$$\begin{aligned} & |q_1^A = 0\rangle \otimes |q_0^A = 0\rangle \otimes |\psi\rangle \\ \mapsto & |0\rangle \otimes |1\rangle \otimes \tilde{n}_{p\sigma}|\psi\rangle + |1\rangle \otimes |0\rangle \otimes n_{p\sigma}|\psi\rangle \equiv |\Phi_{p\sigma}\rangle, \end{aligned} \quad (15)$$

since $(a_{p\sigma}^\dagger)^2$ and $a_{p\sigma}^2$ vanish due to the Fermi statistics. The projective measurement[1] on $|q_0^A\rangle$ is represented by the two operators $\mathcal{P}_q = I \otimes |q\rangle\langle q| \otimes I$ ($q = 0, 1$). The state of the whole system collapses immediately after the measurement as follows:

$$\begin{aligned} |\Phi_{p\sigma}\rangle \xrightarrow{|0\rangle \text{ observed}} & |1\rangle \otimes |0\rangle \otimes \frac{n_{p\sigma}}{\sqrt{\mathbb{P}_{p\sigma}}}|\psi\rangle \\ \text{prob. } \|n_{p\sigma}|\psi\rangle\|^2 & \equiv \mathbb{P}_{p\sigma}, \end{aligned} \quad (16)$$

$$\begin{aligned} |\Phi_{p\sigma}\rangle \xrightarrow{|1\rangle \text{ observed}} & |0\rangle \otimes |1\rangle \otimes \frac{\tilde{n}_{p\sigma}}{\sqrt{\tilde{\mathbb{P}}_{p\sigma}}}|\psi\rangle \\ \text{prob. } \|\tilde{n}_{p\sigma}|\psi\rangle\|^2 & \equiv \tilde{\mathbb{P}}_{p\sigma}. \end{aligned} \quad (17)$$

2. Circuits for off-diagonal components

For mutually different combinations (p, σ) and (p', σ') of spatial orbitals and spins, we define the four non-Hermitian auxiliary operators

$$n_{p\sigma, p'\sigma'}^\pm \equiv \frac{n_{p\sigma} \pm e^{i\pi/4} n_{p'\sigma'}}{2} \quad (18)$$

and

$$\tilde{n}_{p\sigma, p'\sigma'}^\pm \equiv \frac{\tilde{n}_{p\sigma} \pm e^{i\pi/4} \tilde{n}_{p'\sigma'}}{2}. \quad (19)$$

Unnormalized auxiliary states $|\Psi_{p\sigma, p'\sigma'}^\pm\rangle \equiv n_{p\sigma, p'\sigma'}^\pm |\Psi_{gs}\rangle$ can have overlaps $T_{\lambda p\sigma, p'\sigma'}^\pm \equiv |\langle \Psi_\lambda | \Psi_{p\sigma, p'\sigma'}^\pm \rangle|^2$ with the energy eigenstates, from which the charge-charge transition matrix elements in eq. (2) can be calculated as

$$\begin{aligned} N_{\lambda p\sigma, p'\sigma'} &= e^{-i\pi/4} (T_{\lambda p\sigma, p'\sigma'}^+ - T_{\lambda p\sigma, p'\sigma'}^-) \\ &+ e^{i\pi/4} (T_{\lambda p'\sigma', p\sigma}^+ - T_{\lambda p'\sigma', p\sigma}^-). \end{aligned} \quad (20)$$

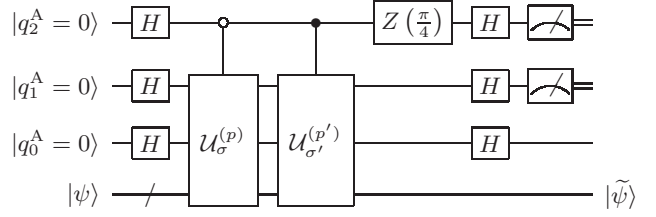


FIG. 2. Charge-charge off-diagonal circuit $\mathcal{C}_{p\sigma, p'\sigma'}$ ($\sigma, \sigma' = \alpha, \beta$) for probabilistic preparation of $n_{p\sigma, p'\sigma'}^\pm |\psi\rangle$ and $\tilde{n}_{p\sigma, p'\sigma'}^\pm |\psi\rangle$ from an arbitrary input state $|\psi\rangle$ and three ancillary qubits. $Z(\pm\pi/4) = \text{diag}(1, e^{\pm i\pi/4})$ is a phase gate. The partial circuits defined in Fig. 1 are contained as the controlled subroutines.

We construct a circuit $\mathcal{C}_{p\sigma, p'\sigma'}$ equipped with three ancillary qubits by using the controlled operations of the partial circuits $\mathcal{U}_\sigma^{(p)}$ and $\mathcal{U}_{\sigma'}^{(p')}$, defined in Fig. 1, as depicted in Fig. 2. The whole system consists of the ancillae and an arbitrary input register $|\psi\rangle$. Its state changes by undergoing the circuit as

$$\begin{aligned} & |q_2^A = 0\rangle \otimes |q_1^A = 0\rangle \otimes |q_0^A = 0\rangle \otimes |\psi\rangle \\ \mapsto & |0\rangle \otimes |0\rangle \otimes |1\rangle \otimes \tilde{n}_{p\sigma, p'\sigma'}^+ |\psi\rangle \\ & + |0\rangle \otimes |1\rangle \otimes |0\rangle \otimes n_{p\sigma, p'\sigma'}^+ |\psi\rangle \\ & + |1\rangle \otimes |0\rangle \otimes |1\rangle \otimes \tilde{n}_{p\sigma, p'\sigma'}^- |\psi\rangle \\ & + |1\rangle \otimes |1\rangle \otimes |0\rangle \otimes n_{p\sigma, p'\sigma'}^- |\psi\rangle \\ \equiv & |\Phi_{p\sigma, p'\sigma'}\rangle. \end{aligned} \quad (21)$$

The projective measurement on $|q_2^A\rangle$ and $|q_1^A\rangle$ is represented by the four operators $\mathcal{P}_{qq'} = |q\rangle\langle q| \otimes |q'\rangle\langle q'| \otimes I \otimes I$ ($q, q' = 0, 1$). The two outcomes among the possible four are of our interest, immediately after which the whole system collapses as follows:

$$\begin{aligned} |\Phi_{p\sigma, p'\sigma'}\rangle \xrightarrow{|0\rangle \otimes |1\rangle \text{ observed}} & |0\rangle \otimes |1\rangle \otimes |0\rangle \otimes \frac{n_{p\sigma, p'\sigma'}^+}{\sqrt{\mathbb{P}_{p\sigma, p'\sigma'}^+}} |\psi\rangle \\ \text{prob. } \|n_{p\sigma, p'\sigma'}^+ |\psi\rangle\|^2 & \equiv \mathbb{P}_{p\sigma, p'\sigma'}^+, \end{aligned} \quad (22)$$

$$\begin{aligned} |\Phi_{p\sigma, p'\sigma'}\rangle \xrightarrow{|1\rangle \otimes |1\rangle \text{ observed}} & |1\rangle \otimes |1\rangle \otimes |0\rangle \otimes \frac{n_{p\sigma, p'\sigma'}^-}{\sqrt{\mathbb{P}_{p\sigma, p'\sigma'}^-}} |\psi\rangle \\ \text{prob. } \|n_{p\sigma, p'\sigma'}^- |\psi\rangle\|^2 & \equiv \mathbb{P}_{p\sigma, p'\sigma'}^-. \end{aligned} \quad (23)$$

3. Transition matrices via statistical sampling

Given the result of a measurement on the ancillary bits for a diagonal or a off-diagonal component, we have the register $|\psi\rangle$ different from the input N -electron state. Then we perform QPE for the Hamiltonian \mathcal{H} by inputting $|\tilde{\psi}\rangle$ to obtain one of the energy eigenvalues in the

Hilbert subspace for the N -electron states. A QPE experiment inevitably suffers from probabilistic errors that depend on the number of qubits and the various parameters for the Suzuki–Trotter decomposition of \mathcal{H} . We assume for simplicity, however, that the QPE procedure is realized on a quantum computer with ideal precision as well as in our previous study.[19] We will thus find the estimated value to be E_λ^N with a probability $|\langle \Psi_\lambda | \tilde{\psi} \rangle|^2$. [1]

If we input $|\Psi_{\text{gs}}\rangle$ to the diagonal circuit $\mathcal{C}_{p\sigma}$ in Fig. 1 and observe the ancillary bit $|q_0^A = 0\rangle$ for QPE, the energy eigenvalue E_λ^N will be obtained with a probability [see eq. (16)]

$$\left| \langle \Psi_\lambda | \frac{n_{p\sigma}}{\sqrt{\mathbb{P}_{p\sigma}}} | \Psi_{\text{gs}} \rangle \right|^2 \mathbb{P}_{p\sigma} = N_{\lambda p\sigma, p\sigma}. \quad (24)$$

This means that we can get the diagonal components of transition matrices N_λ via statistical sampling for a fixed combination of p and σ .

If we input $|\Psi_{\text{gs}}\rangle$ to the off-diagonal circuit $\mathcal{C}_{p\sigma, p'\sigma'}$ in Fig. 2 and observe the ancillary bits $|q_2^A = 0\rangle \otimes |q_1^A = 1\rangle$ or $|q_2^A = 1\rangle \otimes |q_1^A = 1\rangle$ for QPE, the energy eigenvalue E_λ^N will be obtained with probabilities [see eqs. (22) and (23)]

$$\left| \langle \Psi_\lambda | \frac{n_{p\sigma, p'\sigma'}^\pm}{\sqrt{\mathbb{P}_{p\sigma, p'\sigma'}^\pm}} | \Psi_{\text{gs}} \rangle \right|^2 \mathbb{P}_{p\sigma, p'\sigma'}^\pm = T_{\lambda p\sigma, p'\sigma'}^\pm. \quad (25)$$

This means that we can get the off-diagonal components of N_λ from eq. (20) via statistical sampling for a fixed combination of p, p', σ , and σ' .

C. Spin-spin contributions

Let us next consider the determination of the spin-spin transition matrix elements $S_{\lambda p j, p' j'}$ for $j, j' = x, y$. Those involving the z components of spins can be calculated from N_λ by using the relation $s_{pz} = (n_{p\alpha} - n_{p\beta})/2$.

1. Circuits for diagonal components

From the unitary operators in eqs. (10) and (11) for a combination of a spatial orbital p and a spin σ , we define the following four unitary operators:

$$U_{0x}^{(p)} \equiv U_{0p\alpha} U_{1p\beta}, \quad U_{1x}^{(p)} \equiv -U_{1p\alpha} U_{0p\beta} \quad (26)$$

and

$$U_{0y}^{(p)} \equiv -iU_{0p\alpha} U_{0p\beta}, \quad U_{1y}^{(p)} \equiv iU_{1p\alpha} U_{1p\beta}. \quad (27)$$

With them, the spin operators for the x and y directions are written as

$$s_{pj} = \frac{U_{0j}^{(p)} + U_{1j}^{(p)}}{4} \quad (28)$$

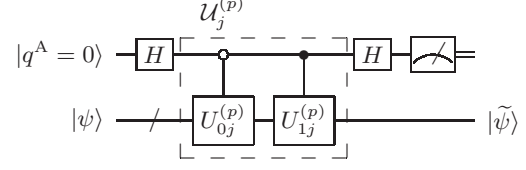


FIG. 3. Spin-spin diagonal circuit \mathcal{C}_{pj} ($j = x, y$) for probabilistic preparation of $s_{pj}|\psi\rangle$ and $\tilde{s}_{pj}|\psi\rangle$ from an arbitrary input state $|\psi\rangle$ and an ancillary qubit. We define the partial circuit $\mathcal{U}_j^{(p)}$ by enclosing it with dashed lines.

for $j = x, y$. We define

$$\tilde{s}_{pj} \equiv \frac{U_{0j}^{(p)} - U_{1j}^{(p)}}{4} \quad (29)$$

for later convenience.

We construct a circuit \mathcal{C}_{pj} equipped with an ancillary qubit by implementing the controlled operations of $U_{0j}^{(p)}$ and $U_{1j}^{(p)}$, as depicted in Fig. 3. The whole system consists of the ancilla and an arbitrary input register $|\psi\rangle$. Its state changes by undergoing the circuit as

$$\begin{aligned} |q^A = 0\rangle \otimes |\psi\rangle &\longmapsto |0\rangle \otimes 2s_{pj}|\psi\rangle + |1\rangle \otimes 2\tilde{s}_{pj}|\psi\rangle \\ &\equiv |\Phi_{pj}\rangle. \end{aligned} \quad (30)$$

The projective measurement on $|q^A\rangle$ is represented by the two operators $\mathcal{P}_q = |q\rangle\langle q| \otimes I$ ($q = 0, 1$). The state of the whole system collapses immediately after the measurement as follows:

$$\begin{aligned} |\Phi_{pj}\rangle &\xrightarrow{|0\rangle \text{ observed}} |0\rangle \otimes \frac{2s_{pj}}{\sqrt{\mathbb{P}_{pj}}} |\psi\rangle \\ \text{prob. } \|2s_{pj}|\psi\rangle\|^2 &\equiv \mathbb{P}_{pj}, \end{aligned} \quad (31)$$

$$\begin{aligned} |\Phi_{pj}\rangle &\xrightarrow{|1\rangle \text{ observed}} |1\rangle \otimes \frac{2\tilde{s}_{pj}}{\sqrt{\tilde{\mathbb{P}}_{pj}}} |\psi\rangle \\ \text{prob. } \|2\tilde{s}_{pj}|\psi\rangle\|^2 &\equiv \tilde{\mathbb{P}}_{pj}. \end{aligned} \quad (32)$$

2. Circuits for off-diagonal components

For mutually different combinations (p, j) and (p', j') of spatial orbitals and spin components $j, j' = x, y$, we define the four non-Hermitian auxiliary operators

$$s_{pj, p'j'}^\pm \equiv \frac{s_{pj} \pm e^{i\pi/4} s_{p'j'}}{2} \quad (33)$$

and

$$\tilde{s}_{pj, p'j'}^\pm \equiv \frac{\tilde{s}_{pj} \pm e^{i\pi/4} \tilde{s}_{p'j'}}{2}. \quad (34)$$

Unnormalized auxiliary states $|\Psi_{pj, p'j'}^\pm\rangle \equiv s_{pj, p'j'}^\pm |\Psi_{\text{gs}}\rangle$ can have overlaps $T_{\lambda pj, p'j'}^\pm \equiv |\langle \Psi_\lambda | \Psi_{pj, p'j'}^\pm \rangle|^2$ with the

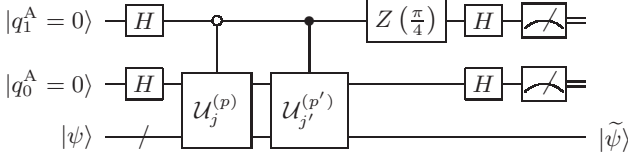


FIG. 4. Spin-spin off-diagonal circuit $\mathcal{C}_{pj,p'j'}$ ($j, j' = x, y$) for probabilistic preparation of $s_{pj,p'j'}^\pm |\psi\rangle$ and $\tilde{s}_{pj,p'j'}^\pm |\psi\rangle$ from an arbitrary input state $|\psi\rangle$ and two ancillary qubits. The partial circuits defined in Fig. 3 are contained as the controlled subroutines.

energy eigenstates, from which the spin-spin transition matrix elements in eq. (3) can be calculated as

$$S_{\lambda pj,p'j'} = e^{-i\pi/4}(T_{\lambda pj,p'j'}^+ - T_{\lambda pj,p'j'}^-) + e^{i\pi/4}(T_{\lambda p'j',pj}^+ - T_{\lambda p'j',pj}^-). \quad (35)$$

We construct a circuit $\mathcal{C}_{pj,p'j'}$ equipped with two ancillary qubits by using the controlled operations of the partial circuits $\mathcal{U}_j^{(p)}$ and $\mathcal{U}_{j'}^{(p')}$, defined in Fig. 3, as depicted in Fig. 4. The whole system consists of the ancillae and an arbitrary input register $|\psi\rangle$. Its state changes by undergoing the circuit as

$$\begin{aligned} & |q_1^A = 0\rangle \otimes |q_0^A = 0\rangle \otimes |\psi\rangle \\ & \mapsto |0\rangle \otimes |0\rangle \otimes 2s_{pj,p'j'}^+ |\psi\rangle \\ & \quad + |0\rangle \otimes |1\rangle \otimes 2\tilde{s}_{pj,p'j'}^+ |\psi\rangle \\ & \quad + |1\rangle \otimes |0\rangle \otimes 2s_{pj,p'j'}^- |\psi\rangle \\ & \quad + |1\rangle \otimes |1\rangle \otimes 2\tilde{s}_{pj,p'j'}^- |\psi\rangle \\ & \equiv |\Phi_{pj,p'j'}\rangle. \end{aligned} \quad (36)$$

The projective measurement on $|q_1^A\rangle$ and $|q_0^A\rangle$ is represented by the four operators $\mathcal{P}_{qq'} = |q\rangle\langle q| \otimes |q'\rangle\langle q'| \otimes I(q, q' = 0, 1)$. The two outcomes among the possible four are of our interest, immediately after which the whole system collapses as follows:

$$\begin{aligned} |\Phi_{pj,p'j'}\rangle & \xrightarrow{|0\rangle \otimes |0\rangle \text{ observed}} |0\rangle \otimes |0\rangle \otimes \frac{2s_{pj,p'j'}^+}{\sqrt{\mathbb{P}_{pj,p'j'}^+}} |\psi\rangle \\ \text{prob.} & \left\| 2s_{pj,p'j'}^+ |\psi\rangle \right\|^2 \equiv \mathbb{P}_{pj,p'j'}^+, \end{aligned} \quad (37)$$

$$\begin{aligned} |\Phi_{pj,p'j'}\rangle & \xrightarrow{|1\rangle \otimes |0\rangle \text{ observed}} |1\rangle \otimes |0\rangle \otimes \frac{2s_{pj,p'j'}^-}{\sqrt{\mathbb{P}_{pj,p'j'}^-}} |\psi\rangle \\ \text{prob.} & \left\| 2s_{pj,p'j'}^- |\psi\rangle \right\|^2 \equiv \mathbb{P}_{pj,p'j'}^-. \end{aligned} \quad (38)$$

3. Transition matrices via statistical sampling

We can get the transition matrices S_λ via statistical sampling similarly to the charge-charge ones. If we input $|\Psi_{\text{gs}}\rangle$ to the diagonal circuit \mathcal{C}_{pj} in Fig. 3 followed by a

measurement and QPE for \mathcal{H} , the energy eigenvalue E_λ will be obtained with a probability $4S_{\lambda pj,pj}$. [See eqs. (3) and (31)] If we use the off-diagonal circuit $\mathcal{C}_{pj,p'j'}$ in Fig. 4, on the other hand, the energy eigenvalue E_λ will be obtained with probabilities $4T_{\lambda pj,p'j'}^\pm$ depending on the measurement outcome. [See eqs. (37) and (38)] The off-diagonal components of transition matrices are then calculated from eq. (35).

D. Spin-charge contributions

Having found ways to determine the charge-charge and spin-spin contributions, let us consider the determination of the spin-charge transition matrices M_λ .

1. Circuits for off-diagonal components

For combinations (p, j) and (p', σ') of spatial orbitals and spin components $j = x, y$ with $\sigma' = \alpha, \beta$, we define the two non-Hermitian auxiliary operators

$$v_{pj,p'\sigma'}^\pm \equiv s_{pj} + e^{\pm i\pi/4} \frac{n_{p'\sigma'}}{2}. \quad (39)$$

Unnormalized auxiliary states $|\Psi_{pj,p'\sigma'}^\pm\rangle \equiv v_{pj,p'\sigma'}^\pm |\Psi_{\text{gs}}\rangle$ can have overlaps $T_{\lambda pj,p'\sigma'}^\pm \equiv |\langle \Psi_\lambda | \Psi_{pj,p'\sigma'}^\pm \rangle|^2$ with the energy eigenstates, from which the spin-charge transition matrix elements in eq. (4) can be calculated as

$$\begin{aligned} M_{\lambda pj,p'\sigma'} & = e^{-i\pi/4} T_{\lambda pj,p'\sigma'}^+ + e^{i\pi/4} T_{\lambda pj,p'\sigma'}^- \\ & \quad - \sqrt{2} S_{\lambda pj,pj} - \frac{N_{\lambda p'\sigma',p'\sigma'}}{2\sqrt{2}}. \end{aligned} \quad (40)$$

We construct a circuit $\mathcal{C}_{pj,p'\sigma'}^\pm$ equipped with three ancillary qubits by using the controlled operations of the partial circuits $\mathcal{U}_j^{(p)}$ in Fig. 3 and $\mathcal{U}_{\sigma'}^{(p')}$ in Fig. 1, as depicted in Fig. 5. The whole system consists of the ancillae and an arbitrary input register $|\psi\rangle$. Its state changes by undergoing the circuit as

$$\begin{aligned} & |q_2^A = 0\rangle \otimes |q_1^A = 0\rangle \otimes |q_0^A = 0\rangle \otimes |\psi\rangle \\ & \mapsto |0\rangle \otimes |0\rangle \otimes |0\rangle \otimes v_{pj,p'\sigma'}^\pm |\psi\rangle \\ & \quad + (|0\rangle \otimes |0\rangle \otimes |1\rangle + |1\rangle \otimes |0\rangle \otimes |1\rangle) \otimes \tilde{s}_{pj} |\psi\rangle \\ & \quad + (|0\rangle \otimes |1\rangle \otimes |1\rangle - |1\rangle \otimes |1\rangle \otimes |1\rangle) \otimes \frac{e^{\pm i\pi/4} \tilde{n}_{p'\sigma'}}{2} |\psi\rangle \\ & \quad + |1\rangle \otimes |0\rangle \otimes |0\rangle \otimes (s_{pj} - e^{\pm i\pi/4} n_{p'\sigma'}) |\psi\rangle \\ & \equiv |\Phi_{pj,p'\sigma'}^\pm\rangle. \end{aligned} \quad (41)$$

The projective measurement on $|q_2^A\rangle$ and $|q_0^A\rangle$ is represented by the four operators $\mathcal{P}_{qq'} = |q\rangle\langle q| \otimes I \otimes |q'\rangle\langle q'| \otimes I(q, q' = 0, 1)$. Only one of the four possible outcomes is of our interest, immediately after which the whole system

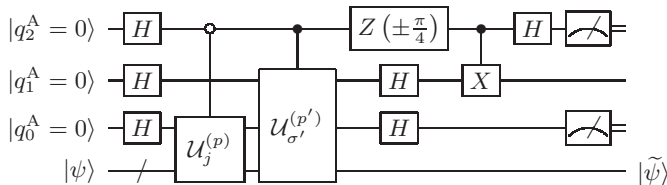


FIG. 5. Spin-charge off-diagonal circuit $C_{pj,p'\sigma'}^\pm$ ($j = x, y$ and $\sigma' = \alpha, \beta$) for probabilistic preparation of $v_{pj,p'\sigma'}^\pm |\psi\rangle$ and other states from an arbitrary input state $|\psi\rangle$ and three ancillary qubits. The partial circuits defined in Figs. 1 and 3 are contained as the controlled subroutines.

collapses as follows:

$$|\Phi_{pj,p'\sigma'}^\pm\rangle^{|0\rangle\otimes|0\rangle\text{observed}} \rightarrow |0\rangle\otimes|0\rangle\otimes|0\rangle\otimes \frac{v_{pj,p'\sigma'}^\pm}{\sqrt{\mathbb{P}_{pj,p'\sigma'}^\pm}} |\psi\rangle$$

$$\text{prob.} \left\| \frac{v_{pj,p'\sigma'}^\pm}{\sqrt{\mathbb{P}_{pj,p'\sigma'}^\pm}} |\psi\rangle \right\|^2 \equiv \mathbb{P}_{pj,p'\sigma'}^\pm. \quad (42)$$

2. Transition matrices via statistical sampling

We can get the transition matrices M_λ via statistical sampling similarly to the charge-charge and spin-spin ones. If we input $|\Psi_{\text{gs}}\rangle$ to the off-diagonal circuit $C_{pj,p'\sigma'}^\pm$ in Fig. 5 followed by a measurement and QPE for \mathcal{H} , the energy eigenvalue E_λ will be obtained with a probability $T_{\lambda pj,p'\sigma'}^\pm$. [See eq. (42)] The off-diagonal components of transition matrices are then calculated from eq. (40).

We provide the pseudocodes in Appendix A for the calculation procedures of response functions explained above.

III. COMPUTATIONAL DETAILS

We adopted STO-6G basis sets as the Cartesian Gaussian-type basis functions[24] for all the elements in our quantum chemistry calculations. The two-electron integrals between the atomic orbitals (AOs) were calculated efficiently.[25] We first performed restricted Hartree-Fock (RHF) calculations to get the orthonormalized molecular orbitals (MOs) in the target systems and calculated the two-electron integrals between them, from which we constructed the second-quantized electronic Hamiltonians.

In the FCI calculations for the large target Hilbert subspaces, we performed exact diagonalization of the electronic (not in qubit representation) Hamiltonians by using the Arnoldi method.[26] We can take the z axis as the quantization axis for spins without loss of generality since our calculations are non-relativistic.

We calculated the FCI response functions simply by substituting the necessary quantities into eq. (9). For the

simulations of response functions from statistical sampling, we generated random numbers according to the matrix elements between the FCI energy eigenstates to mimic the measurements on ancillae and the ideal QPE procedures. We set δ in eq. (9) to 0.01 a.u. throughout the present study.

IV. RESULTS AND DISCUSSION

A. C₂ molecule

We used the experimental bond length of 1.242 Å[27] for a C₂ molecule in the RHF calculation and obtained the total energy $E_{\text{RHF}} = -2045.2939$ eV. This system contains six electrons per spin direction which occupy the lowest six MOs, as shown in Fig. 6(a). We found via the subsequent FCI calculation with $E_{\text{FCI}} = -2052.6918$ eV that the major electronic configuration in the non-degenerate many-electron ground state, denoted by $X^1\Sigma_g^+$ in spectroscopic notation[28], is the same as in the RHF solution. The ground state was found via the exact diagonalization of the Hilbert subspace for $n_\alpha = n_\beta = 6$, from which we obtained the lowest 2000 among the 44100 energy eigenvalues.

We calculated the response functions χ^{FCI} exact within the FCI solution, from which the components $\chi_{1\pi n, 1\pi n}^{\text{FCI}}$ and $\chi_{1\pi z, 3\sigma z}^{\text{FCI}}$ are plotted in Fig. 7. We also performed simulations of statistical sampling for the construction of response function $\chi^{\text{FCI-stat}}$ based on our scheme and plotted those for $N_{\text{meas}} = 10000$ and 40000. It is seen that $\chi_{1\pi n, 1\pi n}^{\text{FCI}}$ in Fig. 7(a), which involves only the HOMO, is well reproduced by $\chi_{1\pi n, 1\pi n}^{\text{FCI-stat}}$ with $N_{\text{meas}} = 10000$. On the other hand, $\chi_{1\pi z, 3\sigma z}^{\text{FCI}}$ in Fig. 7(b) is not accurately reproduced by $\chi_{1\pi n, 1\pi n}^{\text{FCI-stat}}$ with $N_{\text{meas}} = 10000$. These results mean that the response involving a weak excitation channel requires a large number of measurements for its accurate reproduction, just like the situation for the GFs.[19]

B. N₂ molecule

We used the experimental bond length of 1.098 Å[29] for an N₂ molecule in the RHF calculation and obtained the total energy $E_{\text{RHF}} = -2953.5952$ eV. This system contains seven electrons per spin direction which occupy the lowest seven MOs, as shown in Fig. 6(b). We found via the subsequent FCI calculation with $E_{\text{FCI}} = -2957.9124$ eV that the major electronic configuration in the non-degenerate many-electron ground state is $X^1\Sigma_g^+$ [28], the same as in the RHF solution. The ground state was found via the exact diagonalization of the Hilbert subspace for $n_\alpha = n_\beta = 7$, from which we obtained the lowest 2000 among the 14400 energy eigenvalues.

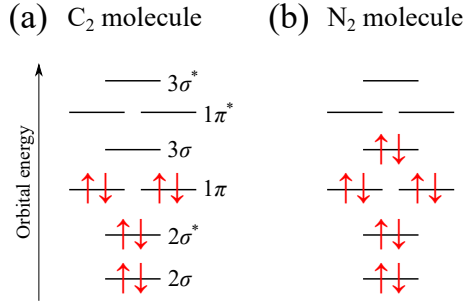


FIG. 6. Schematic illustration of RHF orbitals and their electronic occupancies for (a) a C_2 molecule and (b) an N_2 molecule. The descriptions beside the energy levels represent the orbital characters. Those with asterisks are the anti-bonding orbitals. The 1σ and $1\sigma^*$ MOs, coming from the $1s$ AOs of the constituent atoms, are not shown. The 1π and $1\pi^*$ MOs come mainly from the π bonding of $2p$ AOs, while the 3σ and $3\sigma^*$ MOs from the σ bonding of $2p$ AOs. The non-degenerate many-electron ground state for each system consists mainly of the same electronic configuration as the RHF one.

We calculated the response functions from the FCI solution, from which the components $\chi_{3\sigma n, 3\sigma n}^{\text{FCI}}$ and $\chi_{3\sigma n, 1\pi^* n}^{\text{FCI}}$ are plotted in Fig. 8. We also performed simulations for the construction of $\chi^{\text{FCI-stat}}$ and plotted those for $N_{\text{meas}} = 10000$ and 40000 . It is seen that $\chi_{3\sigma n, 3\sigma n}^{\text{FCI}}$ in Fig. 8(a), which involves only the HOMO, is not well reproduced by $\chi_{3\sigma n, 3\sigma n}^{\text{FCI-stat}}$ with $N_{\text{meas}} = 10000$, in contrast to the C_2 molecule case. Since the strength of $\chi_{3\sigma n, 1\pi^* n}^{\text{FCI}}$ in Fig. 8(b) is similar to that of $\chi_{3\sigma n, 3\sigma n}^{\text{FCI}}$, $N_{\text{meas}} = 10000$ is not sufficient for the accurate reproduction of correct values as well. We found that $\chi_{3\sigma z, 1\pi^* z}^{\text{FCI}}$ (not shown) is much weaker and even $N_{\text{meas}} = 40000$ is insufficient for obtaining good $\chi_{3\sigma z, 1\pi^* z}^{\text{FCI-stat}}$.

V. CONCLUSIONS

We proposed a scheme for the construction of charge and spin linear-response functions of an interacting electronic system via QPE and statistical sampling on a quantum computer. By using the unitary decomposition of electronic operators for avoiding the difficulty due to their non-unitarity, we provided the circuits equipped with at most three ancillae for probabilistic preparation of qubit states on which the necessary non-unitary operators have acted. We performed simulations of such construction of the response functions for C_2 and N_2 molecules by comparing with the accurate ones based on the FCI calculations. It was found that the accurate detection of subtle structures coming from the weak poles in the response functions requires a large number of measurements.

Since the unitary decomposition of electronic operators is applicable regardless of the adopted qubit representa-

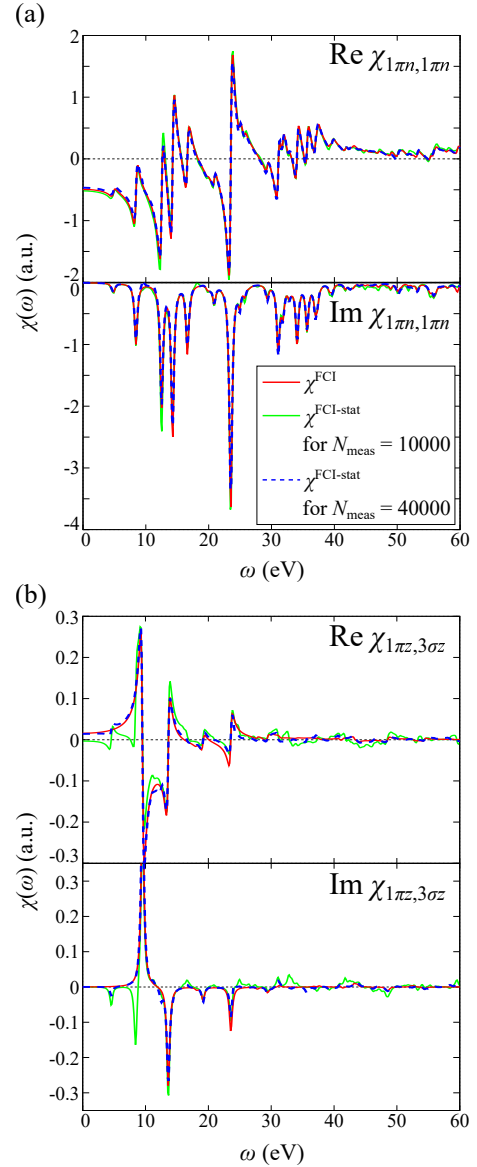


FIG. 7. The response function (a) $\chi_{1\pi n, 1\pi n}^{\text{FCI}}$ and (b) $\chi_{1\pi z, 3\sigma z}^{\text{FCI}}$ exact within the FCI solution for a C_2 molecule. The simulated ones $\chi^{\text{FCI-stat}}$ for for the number of measurements $N_{\text{meas}} = 10000$ and 40000 are also shown.

tion, an electronic state on which an arbitrary product of the creation and annihilation operators has acted can be prepared at least probabilistically. The approach described in this study thus enables one to access not only the response functions and GFs but also various physical quantities on a quantum computer. Invention and enrichment of tools for such properties will enhance the practical use of quantum computers for material simulations.

ACKNOWLEDGMENTS

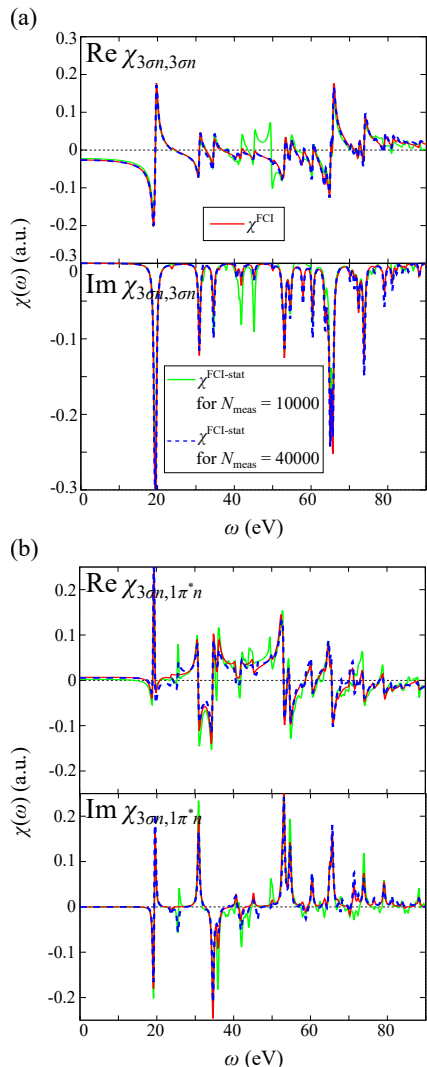


FIG. 8. The response function (a) $\chi_{3\sigma n,3\sigma n}^{\text{FCI}}$ and (b) $\chi_{3\sigma n,1\pi^* n}^{\text{FCI}}$ exact within the FCI solution for an N_2 molecule. The simulated ones $\chi^{\text{FCI-stat}}$ for the number of measurements $N_{\text{meas}} = 10000$ and 40000 are also shown.

This research was supported by MEXT as Exploratory Challenge on Post-K computer (Frontiers of Basic Science: Challenging the Limits) and Grants-in-Aid for Scientific Research (A) (Grant Numbers 18H03770) from JSPS (Japan Society for the Promotion of Science).

Appendix A: Pseudocodes

Here we provide the pseudocodes for the calculation of response functions proposed in the present study. We assume that all the energy eigenvalues of N -electron states have been obtained before entering the main procedure given just below.

1. Main procedure

Here is the main procedure. It calls directly or indirectly all the other procedures provided in this Appendix.

Procedure 1 Calculation of charge and spin response functions via statistical sampling

Input:

Hamiltonian \mathcal{H} , number of spatial orbitals n_{orbs} , N -electron ground state $|\Psi_{\text{gs}}\rangle$ with its energy E_{gs}^N , energy eigenvalues E_{λ}^N , real frequency ω , small positive constant δ , number of measurements N_{meas} for each component

Output:

Response functions $\chi(\omega)$

```

1: function CALCRESPFUNCS( $\mathcal{H}, n_{\text{orbs}}, |\Psi_{\text{gs}}\rangle, E_{\text{gs}}^N, E^N, \omega, \delta, N_{\text{meas}}$ )
2:   for  $\lambda$ 
3:      $d_{\lambda\pm} := \pm(\omega + i\delta) - (E_{\lambda}^N - E_{\text{gs}}^N)$ 
4:    $\chi^{\text{tmp}} := 0$ 
5:   for  $p = 1, \dots, n_{\text{orbs}}$  ▷ Diagonal components
6:     for  $\sigma = \alpha, \beta$  ▷ Charge-charge contributions
7:        $N_{p\sigma, p\sigma} := \text{AmplsChargeDiag}(\mathcal{H}, |\Psi_{\text{gs}}\rangle, E^N, p, \sigma, N_{\text{meas}})$ 
8:       for  $\lambda$ 
9:          $\chi_{p\sigma, p\sigma}^{\text{tmp}} += N_{\lambda p\sigma, p\sigma} / d_{\lambda+} + N_{\lambda p\sigma, p\sigma} / d_{\lambda-}$ 
10:      for  $j = x, y$  ▷ Spin-spin contributions
11:         $S_{pj, pj} := \text{AmplsSpinDiag}(\mathcal{H}, |\Psi_{\text{gs}}\rangle, E^N, p, j, N_{\text{meas}})$ 
12:        for  $\lambda$ 
13:           $\chi_{pj, pj}^{\text{tmp}} += S_{\lambda pj, pj} / d_{\lambda+} + S_{\lambda pj, pj} / d_{\lambda-}$ 
14:      for  $p, p' = 1, \dots, n_{\text{orbs}}$  ( $p \geq p'$ ) ▷ Off-Diagonal components
15:        for  $\sigma, \sigma' = \alpha, \beta$  ▷ Charge-charge contributions
16:          if  $p > p'$  or ( $p == p'$  and  $\sigma == \beta$  and  $\sigma' == \alpha$ ) then
17:             $N_{p\sigma, p'\sigma'} := \text{AmplsChargeOffDiag}(\mathcal{H}, |\Psi_{\text{gs}}\rangle, E^N, p, p', \sigma, \sigma', N_{\text{meas}})$ 
18:            for  $\lambda$ 
19:               $\chi_{p\sigma, p'\sigma'}^{\text{tmp}} += N_{\lambda p\sigma, p'\sigma'} / d_{\lambda+} + N_{\lambda p\sigma, p'\sigma'}^* / d_{\lambda-}, \chi_{p'\sigma', p\sigma}^{\text{tmp}} += N_{\lambda p\sigma, p'\sigma'}^* / d_{\lambda+} + N_{\lambda p\sigma, p'\sigma'} / d_{\lambda-}$ 
20:            for  $j, j' = x, y$  ▷ Spin-spin contributions
21:              if  $p > p'$  or ( $p == p'$  and  $j == y$  and  $j' == x$ ) then
22:                 $S_{pj, p'j'} := \text{AmplsSpinOffDiag}(\mathcal{H}, |\Psi_{\text{gs}}\rangle, E^N, p, p', j, j', N_{\text{meas}})$ 
23:                for  $\lambda$ 
24:                   $\chi_{pj, p'j'}^{\text{tmp}} += S_{\lambda pj, p'j'} / d_{\lambda+} + S_{\lambda pj, p'j'}^* / d_{\lambda-}, \chi_{p'j', pj}^{\text{tmp}} += S_{\lambda pj, p'j'}^* / d_{\lambda+} + S_{\lambda pj, p'j'} / d_{\lambda-}$ 
25:                for  $j = x, y, \sigma' = \alpha, \beta$  ▷ Spin-charge contributions
26:                   $M_{pj, p'\sigma'} := \text{AmplsSpinChargeOffDiag}(\mathcal{H}, |\Psi_{\text{gs}}\rangle, E^N, p, p', j, \sigma', S_{pj, pj}, N_{p'\sigma', p'\sigma'}, N_{\text{meas}})$ 
27:                  for  $\lambda$ 
28:                     $\chi_{pj, p'\sigma'}^{\text{tmp}} += M_{\lambda pj, p'\sigma'} / d_{\lambda+} + M_{\lambda pj, p'\sigma'}^* / d_{\lambda-}, \chi_{p'\sigma', pj}^{\text{tmp}} += M_{\lambda pj, p'\sigma'}^* / d_{\lambda+} + M_{\lambda pj, p'\sigma'} / d_{\lambda-}$ 
29:                ▷ Representation for  $(n, x, y, z)$  from  $(\alpha, \beta, x, y)$ 
30:                 $\chi_{pn, p'n} := \chi_{p\alpha, p'\alpha}^{\text{tmp}} + \chi_{p\alpha, p'\beta}^{\text{tmp}} + \chi_{p\beta, p'\alpha}^{\text{tmp}} + \chi_{p\beta, p'\beta}^{\text{tmp}}, \chi_{pn, p'z} := (\chi_{p\alpha, p'\alpha}^{\text{tmp}} - \chi_{p\alpha, p'\beta}^{\text{tmp}} + \chi_{p\beta, p'\alpha}^{\text{tmp}} - \chi_{p\beta, p'\beta}^{\text{tmp}}) / 2$ 
31:                 $\chi_{pz, p'n} := (\chi_{p\alpha, p'\alpha}^{\text{tmp}} + \chi_{p\alpha, p'\beta}^{\text{tmp}} - \chi_{p\beta, p'\alpha}^{\text{tmp}} - \chi_{p\beta, p'\beta}^{\text{tmp}}) / 2, \chi_{pz, p'z} := (\chi_{p\alpha, p'\alpha}^{\text{tmp}} - \chi_{p\alpha, p'\beta}^{\text{tmp}} - \chi_{p\beta, p'\alpha}^{\text{tmp}} + \chi_{p\beta, p'\beta}^{\text{tmp}}) / 4$ 
32:                for  $j = x, y$ 
33:                   $\chi_{pn, p'j} := \chi_{p\alpha, p'j}^{\text{tmp}} + \chi_{p\beta, p'j}^{\text{tmp}}, \chi_{pz, p'j} := (\chi_{p\alpha, p'j}^{\text{tmp}} - \chi_{p\beta, p'j}^{\text{tmp}}) / 2$ 
34:                   $\chi_{pj, p'n} := \chi_{pj, p'\alpha}^{\text{tmp}} + \chi_{pj, p'\beta}^{\text{tmp}}, \chi_{pj, p'z} := (\chi_{pj, p'\alpha}^{\text{tmp}} - \chi_{pj, p'\beta}^{\text{tmp}}) / 2$ 
35:                for  $j, j' = x, y$ 
36:                   $\chi_{pj, p'j'} := \chi_{pj, p'j'}^{\text{tmp}}$ 
37:      return  $\chi$ 

```

2. Charge-charge contributions

The following procedures calculate the matrix elements in the manner described in Subsection II B.

a. Diagonal components

Procedure 2 Calculation of diagonal components of transition matrices

```

1: function AMPLSCHARGEDIAG( $\mathcal{H}$ ,  $|\Psi_{\text{gs}}\rangle$ ,  $E^N$ ,  $p$ ,  $\sigma$ ,  $N_{\text{meas}}$ )
2:    $N_{p\sigma, p\sigma} := 0$ 
3:   for  $m = 1, \dots, N_{\text{meas}}$ 
4:     Input  $|\Psi_{\text{gs}}\rangle$  to  $\mathcal{C}_{p\sigma}$  and measure the ancilla  $|q_0^A\rangle$  ▷ Circuit in Fig. 1
5:     if  $|q_0^A\rangle == |0\rangle$  then
6:        $E := \text{QPE}(|\tilde{\Psi}\rangle, \mathcal{H})$ , Find  $E$  among  $\{E_\lambda^N\}_\lambda$  ▷ For the register  $|\tilde{\Psi}\rangle$  coming out of the circuit
7:        $N_{\lambda p\sigma, p\sigma} += 1$ 
8:    $N_{p\sigma, p\sigma} *= 1/N_{\text{meas}}$ 
9:   return  $N_{p\sigma, p\sigma}$ 

```

b. Off-diagonal components

Procedure 3 Calculation of off-diagonal components of transition matrices

```

1: function AMPLSCHARGEOFFDIAG( $\mathcal{H}$ ,  $|\Psi_{\text{gs}}\rangle$ ,  $E^N$ ,  $p$ ,  $p'$ ,  $\sigma$ ,  $\sigma'$ ,  $N_{\text{meas}}$ )
2:    $T_{p\sigma, p'\sigma'}^\pm := \text{AmplsChargeAux}(\mathcal{H}, |\Psi_{\text{gs}}\rangle, E^N, p, p', \sigma, \sigma', N_{\text{meas}})$ 
3:    $T_{p'\sigma', p\sigma}^\pm := \text{AmplsChargeAux}(\mathcal{H}, |\Psi_{\text{gs}}\rangle, E^N, p', p, \sigma', \sigma, N_{\text{meas}})$ 
4:   for  $\lambda$ 
5:      $N_{\lambda p\sigma, p'\sigma'} := e^{-i\pi/4}(T_{\lambda p\sigma, p'\sigma'}^+ - T_{\lambda p\sigma, p'\sigma'}^-) + e^{i\pi/4}(T_{\lambda p'\sigma', p\sigma}^+ - T_{\lambda p'\sigma', p\sigma}^-)$  ▷ See eq. (20)
6:   return  $N_{p\sigma, p'\sigma'}$ 

```

Procedure 4 Calculation of transition amplitudes for auxiliary states

```

1: function AMPLSCHARGEAux( $\mathcal{H}$ ,  $|\Psi_{\text{gs}}^N\rangle$ ,  $E^N$ ,  $p$ ,  $p'$ ,  $\sigma$ ,  $\sigma'$ ,  $N_{\text{meas}}$ )
2:    $T_{p\sigma, p'\sigma'}^\pm := 0$ 
3:   for  $m = 1, \dots, N_{\text{meas}}$ 
4:     Input  $|\Psi_{\text{gs}}\rangle$  to  $\mathcal{C}_{p\sigma, p'\sigma'}$  and measure the ancillae  $|q_2^A\rangle$  and  $|q_1^A\rangle$  ▷ Circuit in Fig. 2
5:     if  $|q_2^A\rangle \otimes |q_1^A\rangle == |0\rangle \otimes |1\rangle$  then
6:        $E := \text{QPE}(|\tilde{\Psi}\rangle, \mathcal{H})$ , Find  $E$  among  $\{E_\lambda^N\}_\lambda$  ▷ For the register  $|\tilde{\Psi}\rangle$  coming out of the circuit
7:        $T_{\lambda p\sigma, p'\sigma'}^+ += 1$ 
8:     else if  $|q_2^A\rangle \otimes |q_1^A\rangle == |1\rangle \otimes |1\rangle$  then
9:        $E := \text{QPE}(|\tilde{\Psi}\rangle, \mathcal{H})$ , Find  $E$  among  $\{E_\lambda^N\}_\lambda$  ▷ For the register  $|\tilde{\Psi}\rangle$  coming out of the circuit
10:       $T_{\lambda p\sigma, p'\sigma'}^- += 1$ 
11:    $T_{p\sigma, p'\sigma'}^\pm *= 1/N_{\text{meas}}$ 
12:   return  $T_{p\sigma, p'\sigma'}^\pm$ 

```

3. Spin-spin contributions

The following procedures calculate the matrix elements in the manner described in Subsection II C.

a. Diagonal components

Procedure 5 Calculation of diagonal components of transition matrices

```

1: function AMPLSPINDIAG( $\mathcal{H}, |\Psi_{\text{gs}}\rangle, E^N, p, j, N_{\text{meas}}$ )
2:    $S_{pj,pj} := 0$ 
3:   for  $m = 1, \dots, N_{\text{meas}}$ 
4:     Input  $|\Psi_{\text{gs}}\rangle$  to  $\mathcal{C}_{pj}$  and measure the ancilla  $|q^A\rangle$  ▷ Circuit in Fig. 3
5:     if  $|q^A\rangle == |0\rangle$  then
6:        $E := \text{QPE}(|\tilde{\Psi}\rangle, \mathcal{H})$ , Find  $E$  among  $\{E_\lambda^N\}_\lambda$  ▷ For the register  $|\tilde{\Psi}\rangle$  coming out of the circuit
7:        $S_{\lambda pj,pj} += 1$ 
8:    $S_{pj,pj} *= 1/(4N_{\text{meas}})$ 
9:   return  $S_{pj,pj}$ 

```

b. Off-diagonal components

Procedure 6 Calculation of off-diagonal components of transition matrices

```

1: function AMPLSPINOFFDIAG( $\mathcal{H}, |\Psi_{\text{gs}}\rangle, E^N, p, p', j, j', N_{\text{meas}}$ )
2:    $T_{pj,p'j'}^\pm := \text{AmplsSpinAux}(\mathcal{H}, |\Psi_{\text{gs}}\rangle, E^N, p, p', j, j', N_{\text{meas}})$ 
3:    $T_{p'j',pj}^\pm := \text{AmplsSpinAux}(\mathcal{H}, |\Psi_{\text{gs}}\rangle, E^N, p', p, j', j, N_{\text{meas}})$ 
4:   for  $\lambda$ 
5:      $S_{\lambda pj,p'j'} := e^{-i\pi/4}(T_{\lambda pj,p'j'}^+ - T_{\lambda pj,p'j'}^-) + e^{i\pi/4}(T_{\lambda p'j',pj}^+ - T_{\lambda p'j',pj}^-)$  ▷ See eq. (35)
6:   return  $S_{pj,p'j'}$ 

```

Procedure 7 Calculation of transition amplitudes for auxiliary states

```

1: function AMPLSPINAUX( $\mathcal{H}, |\Psi_{\text{gs}}\rangle, E^N, p, p', j, j', N_{\text{meas}}$ )
2:    $T_{pj,p'j'}^\pm := 0$ 
3:   for  $m = 1, \dots, N_{\text{meas}}$ 
4:     Input  $|\Psi_{\text{gs}}\rangle$  to  $\mathcal{C}_{pj,p'j'}$  and measure the ancillae  $|q_1^A\rangle$  and  $|q_0^A\rangle$  ▷ Circuit in Fig. 4
5:     if  $|q_1^A\rangle \otimes |q_0^A\rangle == |0\rangle \otimes |0\rangle$  then
6:        $E := \text{QPE}(|\tilde{\Psi}\rangle, \mathcal{H})$ , Find  $E$  among  $\{E_\lambda^N\}_\lambda$  ▷ For the register  $|\tilde{\Psi}\rangle$  coming out of the circuit
7:        $T_{\lambda pj,p'j'}^+ += 1$ 
8:     else if  $|q_1^A\rangle \otimes |q_0^A\rangle == |1\rangle \otimes |0\rangle$  then
9:        $E := \text{QPE}(|\tilde{\Psi}\rangle, \mathcal{H})$ , Find  $E$  among  $\{E_\lambda^N\}_\lambda$  ▷ For the register  $|\tilde{\Psi}\rangle$  coming out of the circuit
10:       $T_{\lambda pj,p'j'}^- += 1$ 
11:    $T_{pj,p'j'}^\pm *= 1/(4N_{\text{meas}})$ 
12:   return  $T_{pj,p'j'}^\pm$ 

```

4. Spin-charge contributions

The following procedures calculate the matrix elements in the manner described in Subsection IID.

Procedure 8 Calculation of off-diagonal components of transition matrices

```

1: function AMPLSPINCHARGEOFFDIAG( $\mathcal{H}, |\Psi_{\text{gs}}\rangle, E^N, p, p', j, \sigma', S_{pj,pj}, N_{p'\sigma',p'\sigma'}, N_{\text{meas}}$ )
2:    $T_{pj,p'\sigma'}^\pm := \text{AmplsSpinChargeAux}(\mathcal{H}, |\Psi_{\text{gs}}\rangle, E^N, \pm, p, p', j, \sigma', N_{\text{meas}})$ 
3:   for  $\lambda$ 
4:      $M_{\lambda pj,p'\sigma'} := e^{-i\pi/4}T_{\lambda pj,p'\sigma'}^+ + e^{i\pi/4}T_{\lambda pj,p'\sigma'}^- - \sqrt{2}S_{\lambda pj,pj} - \frac{N_{\lambda p'\sigma',p'\sigma'}}{2\sqrt{2}}$  ▷ See eq. (40)
5:   return  $M_{pj,p'\sigma'}$ 

```

Procedure 9 Calculation of transition amplitudes for auxiliary states

```

1: function AMPLSPINCHARGEAUX( $\mathcal{H}, |\Psi_{gs}\rangle, E^N, \nu, p, p', j, \sigma', N_{\text{meas}}$ )
2:    $T_{pj,p'\sigma'}^\nu := 0$ 
3:   for  $m = 1, \dots, N_{\text{meas}}$ 
4:     Input  $|\Psi_{gs}\rangle$  to  $C_{pj,p'\sigma'}^\nu$  and measure the ancillae  $|q_2^\Delta\rangle$  and  $|q_0^\Delta\rangle$  ▷ Circuit in Fig. 5
5:     if  $|q_2^\Delta\rangle \otimes |q_0^\Delta\rangle == |0\rangle \otimes |0\rangle$  then
6:        $E := \text{QPE}(|\tilde{\Psi}\rangle, \mathcal{H})$ , Find  $E$  among  $\{E_\lambda^N\}_\lambda$  ▷ For the register  $|\tilde{\Psi}\rangle$  coming out of the circuit
7:        $T_{\lambda pj,p'\sigma'}^\nu += 1$ 
8:    $T_{pj,p'\sigma'}^\nu *= 1/N_{\text{meas}}$ 
9:   return  $T_{pj,p'\sigma'}^\nu$ 

```

- [1] M. A. Nielsen and I. L. Chuang, *Quantum Computation and Quantum Information: 10th Anniversary Edition*, 10th ed. (Cambridge University Press, New York, NY, USA, 2011).
- [2] F. Arute, K. Arya, R. Babbush, D. Bacon, J. C. Bardin, R. Barends, R. Biswas, S. Boixo, F. G. S. L. Brandao, D. A. Buell, B. Burkett, Y. Chen, Z. Chen, B. Chiaro, R. Collins, W. Courtney, A. Dunsworth, E. Farhi, B. Foxen, A. Fowler, C. Gidney, M. Giustina, R. Graff, K. Guerin, S. Habegger, M. P. Harrigan, M. J. Hartmann, A. Ho, M. Hoffmann, T. Huang, T. S. Humble, S. V. Isakov, E. Jeffrey, Z. Jiang, D. Kafri, K. Kechedzhi, J. Kelly, P. V. Klimov, S. Knysh, A. Korotkov, F. Kostritsa, D. Landhuis, M. Lindmark, E. Lucero, D. Lyakh, S. Mandra, J. R. McClean, M. McEwen, A. Megrant, X. Mi, K. Michielsen, M. Mohseni, J. Mutus, O. Naaman, M. Neeley, C. Neill, M. Y. Niu, E. Ostby, A. Petukhov, J. C. Platt, C. Quintana, E. G. Rieffel, P. Roushan, N. C. Rubin, D. Sank, K. J. Satzinger, V. Smelyanskiy, K. J. Sung, M. D. Trevithick, A. Vainsencher, B. Villalonga, T. White, Z. J. Yao, P. Yeh, A. Zalcman, H. Neven, and J. M. Martinis, *Nature* **574**, 505 (2019).
- [3] S. McArdle, S. Endo, A. Aspuru-Guzik, S. Benjamin, and X. Yuan, arXiv e-prints , arXiv:1808.10402 (2018), arXiv:1808.10402 [quant-ph].
- [4] P. Jordan and E. Wigner, *Zeitschrift für Physik* **47**, 631 (1928).
- [5] S. B. Bravyi and A. Y. Kitaev, *Annals of Physics* **298**, 210 (2002).
- [6] A. Aspuru-Guzik, A. D. Dutoi, P. J. Love, and M. Head-Gordon, *Science* **309**, 1704 (2005), <https://science.sciencemag.org/content/309/5741/1704.full.pdf>
- [7] A. Peruzzo, J. McClean, P. Shadbolt, M.-H. Yung, X.-Q. Zhou, P. J. Love, A. Aspuru-Guzik, and J. L. O'Brien, *Nature Communications* **5**, 4213 EP (2014), article.
- [8] P. J. J. O'Malley, R. Babbush, I. D. Kivlichan, J. Romero, J. R. McClean, R. Barends, J. Kelly, P. Roushan, A. Tranter, N. Ding, B. Campbell, Y. Chen, Z. Chen, B. Chiaro, A. Dunsworth, A. G. Fowler, E. Jeffrey, E. Lucero, A. Megrant, J. Y. Mutus, M. Neeley, C. Neill, C. Quintana, D. Sank, A. Vainsencher, J. Wenner, T. C. White, P. V. Coveney, P. J. Love, H. Neven, A. Aspuru-Guzik, and J. M. Martinis, *Phys. Rev. X* **6**, 031007 (2016).
- [9] A. Kandala, A. Mezzacapo, K. Temme, M. Takita, M. Brink, J. M. Chow, and J. M. Gambetta, *Nature* **549**, 242 EP (2017).
- [10] C. Hempel, C. Maier, J. Romero, J. McClean, T. Monz, H. Shen, P. Jurcevic, B. P. Lanyon, P. Love, R. Babbush, A. Aspuru-Guzik, R. Blatt, and C. F. Roos, *Phys. Rev. X* **8**, 031022 (2018).
- [11] J. R. McClean, M. E. Kimchi-Schwartz, J. Carter, and W. A. de Jong, *Phys. Rev. A* **95**, 042308 (2017).
- [12] K. M. Nakanishi, K. Mitarai, and K. Fujii, arXiv e-prints , arXiv:1810.09434 (2018), arXiv:1810.09434 [quant-ph].
- [13] O. Higgott, D. Wang, and S. Brierley, arXiv e-prints , arXiv:1805.08138 (2018), arXiv:1805.08138 [quant-ph].
- [14] R. Santagati, J. Wang, A. A. Gentile, S. Paesani, N. Wiebe, J. R. McClean, S. Morley-Short, P. J. Shadbolt, D. Bonneau, J. W. Silverstone, D. P. Tew, X. Zhou, J. L. O'Brien, and M. G. Thompson, *Science Advances* **4** (2018), 10.1126/sciadv.aap9646, <https://advances.sciencemag.org/content/4/1/eaap9646.full.pdf>.
- [15] J. I. Colless, V. V. Ramasesh, D. Dahlen, M. S. Blok, M. E. Kimchi-Schwartz, J. R. McClean, J. Carter, W. A. de Jong, and I. Siddiqi, *Phys. Rev. X* **8**, 011021 (2018).
- [16] T. Jones, S. Endo, S. McArdle, X. Yuan, and S. C. Benjamin, *Phys. Rev. A* **99**, 062304 (2019).
- [17] A. Damascelli, *Physica Scripta* **2004**, 61 (2004).
- [18] T. Kosugi and Y.-I. Matsushita, *Journal of Physics: Condensed Matter* **30**, 435604 (2018).
- [19] T. Kosugi and Y.-i. Matsushita, arXiv e-prints , arXiv:1908.03902 (2019), arXiv:1908.03902 [quant-ph].
- [20] S. Endo, I. Kurata, and Y. O. Nakagawa, arXiv e-prints , arXiv:1909.12250 (2019), arXiv:1909.12250 [quant-ph].
- [21] G. Stefanucci and R. van Leeuwen, *Nonequilibrium Many-Body Theory of Quantum Systems* (Cambridge University Press, 2013).
- [22] T. Kosugi and Y.-i. Matsushita, *The Journal of Chemical Physics* **147**, 114105 (2017), <https://doi.org/10.1063/1.4994720>.
- [23] L. Hedin, *Phys. Rev.* **139**, A796 (1965).
- [24] T. Helgaker, P. Jørgensen, and J. Olsen, *Molecular Electronic-Structure Theory* (Wiley, 2000).
- [25] J. T. Fermann and E. F. Valeev, "Libint: Machine-generated library for efficient evaluation of molecular integrals over Gaussians," (2003), freely available at

- <http://libint.valeev.net/> or one of the authors.
- [26] R. Lehoucq, D. Sorensen, and C. Yang, *ARPACK Users' Guide* (Society for Industrial and Applied Mathematics, 1998) <http://epubs.siam.org/doi/pdf/10.1137/1.9780898719628>.
- [27] M. Douay, R. Nietmann, and P. Bernath, *Journal of Molecular Spectroscopy* **131**, 250 (1988).
- [28] L. Bytautas and K. Ruedenberg, *The Journal of Chemical Physics* **122**, 154110 (2005), <https://doi.org/10.1063/1.1869493>.
- [29] L. Sutton, *Tables of Interatomic Distances and Configuration in Molecules and Ions* (The Chemical Society, London, 1958).